JGP Journal of General Physiology

VIEWPOINT

Myosin motors that cannot bind actin leave their folded OFF state on activation of skeletal muscle

Massimo Reconditi[1,2], Elisabetta Brunello[3], Luca Fusi[3], Marco Linari[1], Vincenzo Lombardi[1], Malcolm Irving[3], and Gabriella Piazzesi[1]

The myosin motors in resting skeletal muscle are folded back against their tails in the thick filament in a conformation that makes them unavailable for binding to actin. When muscles are activated, calcium binding to troponin leads to a rapid change in the structure of the actin-containing thin filaments that uncovers the myosin binding sites on actin. Almost as quickly, myosin motors leave the folded state and move away from the surface of the thick filament. To test whether motor unfolding is triggered by the availability of nearby actin binding sites, we measured changes in the x-ray reflections that report motor conformation when muscles are activated at longer sarcomere length, so that part of the thick filaments no longer overlaps with thin filaments. We found that the intensity of the M3 reflection from the axial repeat of the motors along the thick filaments declines almost linearly with increasing sarcomere length up to 2.8 µm, as expected if motors in the nonoverlap zone had left the folded state and become relatively disordered. In a recent article in *JGP*, Squire and Knupp challenged this interpretation of the data. We show here that their analysis is based on an incorrect assumption about how the interference subpeaks of the M3 reflection were reported in our previous paper. We extend previous models of mass distribution along the filaments to show that the sarcomere length dependence of the M3 reflection is consistent with <10% of no-overlap motors remaining in the folded conformation during active contraction, confirming our previous conclusion that unfolding of myosin motors on muscle activation is not due to the availability of local actin binding sites.

Contraction of skeletal and cardiac muscle is triggered by a transient rise in intracellular calcium concentration. Calcium ions bind to regulatory sites on troponin in the actin-containing thin filaments, initiating a change in thin filament structure that exposes binding sites on actin for myosin motors from the overlapping thick filament (Huxley, 1973; Parry and Squire, 1973; Gordon et al., 2000). Until recently, this calcium/thin filament signaling pathway was considered to be a sufficient description of the regulation of contraction in vertebrate striated muscle, although molecular details of thin filament structure and its modulation by calcium binding continued to be elucidated (Yamada et al., 2020).

That exclusively thin filament model of muscle regulation was challenged by a series of structural and biochemical studies of myosin, thick filaments, and muscle cells. An OFF state of myosin was described in smooth muscle myosin and in isolated thick filaments from invertebrate skeletal muscle (Wendt et al., 2001; Woodhead et al., 2005), in which the two motor domains of each myosin molecule are folded back against its tail in the thick filament backbone. A similar folded structure was subsequently seen in isolated thick filaments from mammalian cardiac muscle (Zoghbi et al., 2008; AL-Khayat et al., 2013) and identified in resting intact skeletal muscle fibers of vertebrates by cryo-electron tomography (Luther et al., 2011) and by x-ray interference (Reconditi et al., 2011). A population of myosin motors with extremely low ATP turnover was discovered in resting mammalian skeletal muscle (Stewart et al., 2010) and became identified with the folded state seen in the structural studies (Irving, 2017). Because myosin motors in the folded state are unavailable for actin interaction, these studies led to the conclusion that the well-known calcium/thin filament signaling pathway is a necessary but not sufficient component of the regulation of contraction in skeletal muscle. The same conclusion can be made for the regulation of heart muscle (Hooijman et al., 2011; Reconditi et al., 2017; Brunello et al., 2020).

That conclusion, however, leads to a fundamental question: what controls the release of the myosin motors from the folded OFF state following the calcium transient? Although there may be a population of motors in resting muscle that are not folded and whose function could therefore be regulated by the conventional

[1]PhysioLab, Università di Firenze, Sesto Fiorentino, Italy; [2]Consorzio Nazionale Interuniversitario per le Scienze Fisiche della Materia, Unità di Ricerca Università di Firenze, Florence, Italy; [3]Randall Centre for Cell and Molecular Biophysics, King's College London, London, UK.

Correspondence to Malcolm Irving: malcolm.irving@kcl.ac.uk

This work is part of a special collection on myofilament function and disease.

thin filament mechanism, there is little doubt that the folded motors in resting muscle are released from that state when intact muscles are electrically stimulated. Because they are organized in a quasi-helical array on the surface of the thick filament (Huxley and Brown, 1967; Woodhead et al., 2005), the folded motors give rise to a characteristic x-ray reflection corresponding to a helical periodicity of ∼43 nm called the "first myosin layer line" (ML1; Huxley and Brown, 1967; Haselgrove, 1975), which is lost following electrical stimulation. Moreover, time-resolved x-ray studies on single fibers from skeletal muscle showed that the loss of the folded motors signaled by the ML1 layer line is fast enough to control the attachment of the motors to actin (Reconditi et al., 2011).

It seems unlikely that release of the folded motors from the surface of the thick filaments is directly controlled by the intracellular free calcium transient, because it can be prevented or delayed by imposing rapid shortening at the start of electrical stimulation (Linari et al., 2015). This experiment also suggested that activation of the thick filament is mechanically controlled (i.e., that exit of motors from the folded state is triggered by stress in the thick filament; Linari et al., 2015; Fusi et al., 2016). According to this idea, a population of motors that are not folded in resting muscle could bind to actin when the thin filament is activated and could generate enough active force to activate the folded motors through thick filament mechanosensing. The molecular basis of thick filament mechanosensing remains unknown, however, and the intrinsic positive feedback of the phenomenon makes it likely that additional mechanisms are involved, particularly in the control of muscle relaxation (Brunello et al., 2009; Irving, 2017).

Apart from the myosin motors themselves, the most likely molecular mediator of interfilament signaling in the muscle sarcomere is myosin binding protein C (MyBP-C), a constitutive component of the thick filament whose N-terminus can bind to the thin filament (Shaffer et al., 2009; Luther et al., 2011). MyBP-C is confined to the two "C zones" in each thick filament, from 250 to 510 nm from the filament midpoint in fast-twitch muscles. Because thin filaments are ∼1.0 µm long, the C zones fully overlap the thin filaments at sarcomere lengths less than ∼2.5 µm, and the overlap is gradually reduced as sarcomere length is increased to ∼3.0 µm. We therefore used the sarcomere length dependence of the x-ray diffraction patterns from resting and isometrically contracting skeletal muscle fibers to investigate the hypothetical role of MyBP-C as an interfilament signaling molecule (Reconditi et al., 2014). We found that the intensity of the ML1 layer line, an x-ray signature of the folded motors, was independent of sarcomere length in resting muscle in the range from 2.1 to 2.6 µm, then decreased in the range from 2.6 to 3.0 µm, as expected from the hypothesis that the folded motor conformation is stabilized by an interaction between MyBP-C and the thin filaments in resting muscle. The sarcomere length dependence of the axial periodicity of the thick filament backbone, calculated from the spacing of the sixth-order myosin-based meridional reflection, another x-ray signal that reports the regulatory state of the thick filament, supported that conclusion.

In the same series of experiments, we measured the sarcomere length dependence of the intensity of the M3 x-ray reflection (I_{M3}), corresponding to the ∼14.5-nm axial periodicity of

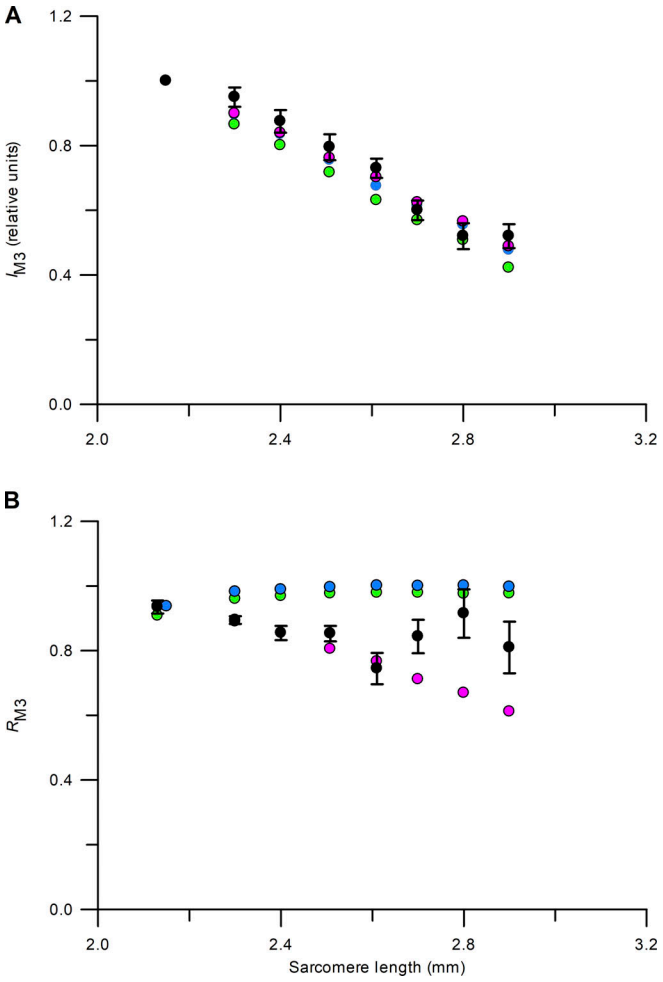

Figure 1. **Sarcomere length dependence of the normalized I_{M3} and the relative intensity of its two central subpeaks (R_{M3}) during isometric contraction.** Black circles show experimental data (mean ± SEM; n = 8) from small bundles of fibers from tibialis anterior muscles of *Rana esculenta* at 4°C (Reconditi et al., 2014). Magenta circles represent the model of Brunello et al. (2007) (in B, magenta points to sarcomere length 2.4 µm coinciding with the experimental data). Green circles represent the modified model in which detached motors make no contribution to the M3 reflection. Blue circles represent the modified model in which 10% of the motors in the no-overlap region are in the folded conformation. See text for details. **(A)** Normalized I_{M3} during isometric contraction. **(B)** Relative intensity of the two central subpeaks during isometric contraction.

the myosin motors along the filaments. I_{M3} is sensitive to the axial mass distribution of the myosin motors (Irving et al., 2000), and we found that it was independent of sarcomere length in resting muscle but decreased almost linearly with increasing sarcomere length in the range from 2.1 to 2.8 µm in isometrically contracting muscle (Fig. 1 A, filled black circles). Thus, like isometric force (Gordon et al., 1966), I_{M3} is proportional to the degree of overlap between the myosin-containing thick and actin-containing thin filaments. The relationship diverged from linearity at sarcomere lengths >2.8 µm, at which sarcomere lengths became heterogeneous (Reconditi et al., 2014). Decreases in the axial alignment between neighboring thick filaments and in the axial periodicity of the thick filament were already detectable at sarcomere lengths >2.6 µm. Our

interpretation of the behavior of I_{M3} in the linear region was that the actin-bound myosin motors in the region of overlap between thick and thin filaments have the high degree of axial order characterized in previous x-ray studies at short sarcomere length (Irving et al., 2000; Piazzesi et al., 2002; Reconditi et al., 2004; Huxley et al., 2006), but the motors in the nonoverlap region that cannot bind to actin are relatively disordered axially. This conclusion constrains possible mechanisms of thick filament regulation, since it implies that myosin motors that have no opportunity to bind to actin because they are outside the region of filament overlap leave the folded OFF conformation following electrical stimulation, independently of whether they are in the C zone.

In a recent article in *JGP*, Squire and Knupp (2021) challenged that interpretation of the sarcomere length dependence of I_{M3} in isometrically contracting muscle. Our interpretation was based on a structural model for the distribution of the mass of the myosin motors along the filaments that we had developed previously to explain the response of skeletal muscle to a quick stretch (Brunello et al., 2007). In that model, each myosin motor takes one of three conformations: actin-attached force-generating motors; their intramolecular partners in the same myosin molecule; and detached (*D*) motors, in which neither of the motor domains in a myosin dimer is attached to actin. The *D* motors are not completely disordered but have a Gaussian axial dispersion of 3.6 nm. It was also assumed that none of the motors were in the folded state during active contraction. To adapt this model to longer sarcomere lengths, we proposed that motors in the region of the thick filament that cannot attach to actin because no thin filament is accessible to them are in the *D* state.

Models of this type are constrained by both the intensity and the detailed axial profile of the M3 reflection (Fig. 2), which is the result of x-ray interference between the two arrays of myosin motors in each centrosymmetric thick filament (Linari et al., 2000). This effect modulates the broad single x-ray reflection that would be generated by the single array of myosin motors in each half thick filament by a fringe pattern with a spatial frequency corresponding to the separation between the two arrays in each filament (Reconditi, 2006). The net result is to split the reflection into a series of closely spaced subpeaks, of which the central two are prominent at short sarcomere length (Fig. 2 A), but the outer peaks become more prominent at longer sarcomere lengths (Fig. 2 B). The separation between the interference subpeaks decreases slightly but significantly with increasing sarcomere length, and the decrease is consistent with that expected from the increase in the separation between the two arrays of actin-attached motors in each thick filament (Linari et al., 2000).

The distribution of the mass of the myosin motors along the filament axis in the models of Brunello et al. (2007) and Reconditi et al. (2014) and described above give a good fit to both the total I_{M3} (Fig. 1 A; black, observed values; magenta, model) from isometrically contracting muscle and the ratio of the intensities of its two most intense subpeaks (higher angle/lower angle, R_{M3}; Fig. 1 B) in the sarcomere length range from 2.1 to 2.6 µm. The experimental and model values of R_{M3} become systematically different at longer sarcomere lengths, at which the

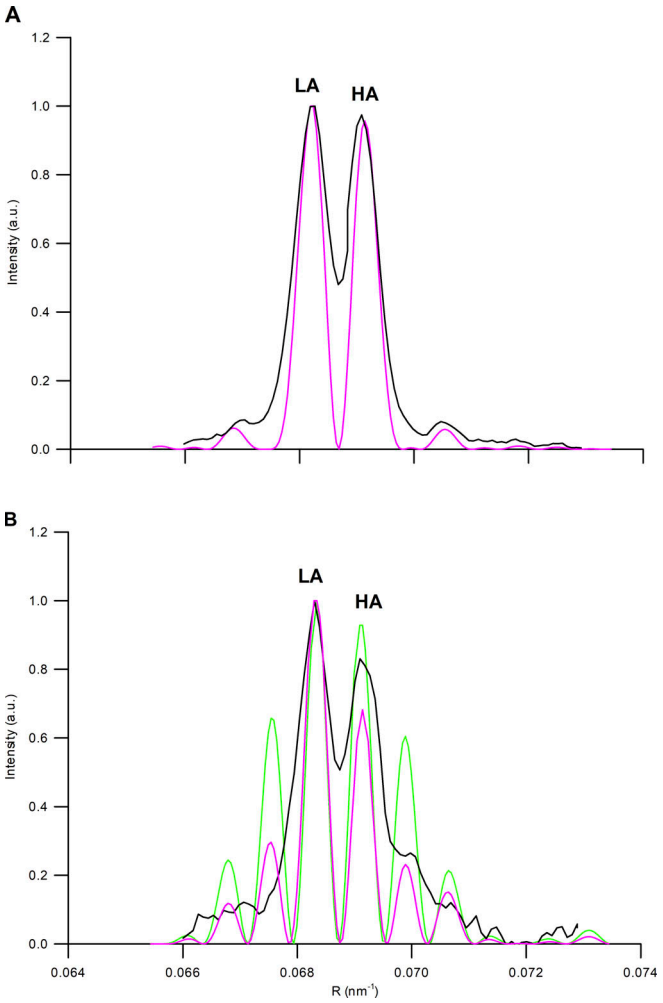

Figure 2. **Axial profile of the M3 reflection during isometric contraction at sarcomere lengths 2.15 µm and 2.90 µm.** Black, experimental profiles reproduced from Reconditi et al. (2014; inset of their Fig. 4 B); magenta, model of Brunello et al. (2007) (green, modified model in which detached motors make no contribution to the M3 reflection). Magenta and green profiles coincide in A. Profiles scaled by the intensity of the lower-angle (LA) central subpeak. R_{M3} in Fig. 1 is the relative intensity of the higher-angle (HA) and LA central subpeaks. **(A)** Sarcomere length 2.15 µm. **(B)** Sarcomere length 2.90 µm. a.u., arbitrary units.

cross-meridional width of the M3 reflection (Fig. 3) starts to increase, indicating axial misalignment between neighboring thick filaments as discussed further below. Reconditi et al. (2014) did not attempt to optimize the fit by altering the published model parameters, but, in checking those calculations, we found that the model values we previously calculated for R_{M3} were slightly too high. This does not affect the conclusion of that paper, that the model of Brunello et al. (2007) in which the nonoverlap motors have a Gaussian axial dispersion of 3.6 nm reproduces the observed dependence of the M3 reflection up to sarcomere length 2.6 µm. Moreover, it provides a better fit than a model in which the nonoverlap motors are so disordered that they make no contribution to the M3 reflection (Fig. 1, A and B, green). The partial order of the motors in the no-overlap region also reduces the relative amplitude of the outer interference

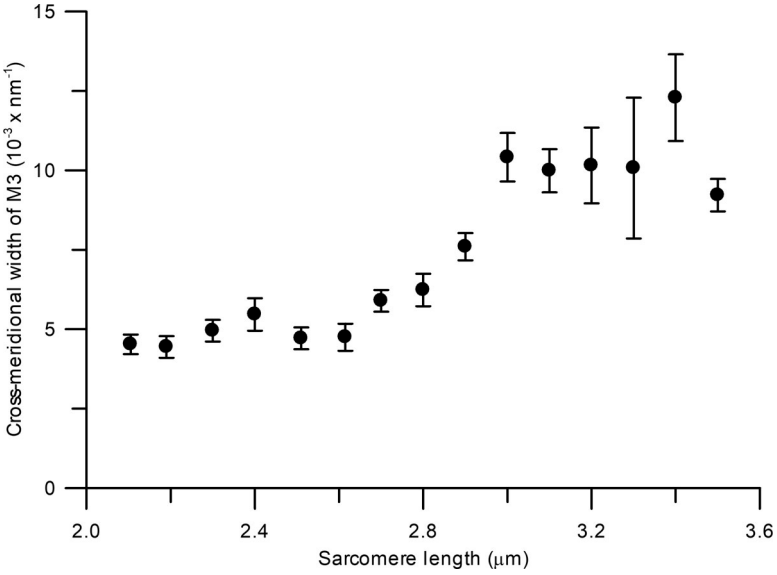

Figure 3. **Sarcomere length dependence of the cross-meridional width of the M3 reflection during isometric contraction.** The cross-meridional width is measured as the SD of the Gaussian curve used to fit the cross-meridional intensity profile. Mean ± SEM from 10–14 fiber bundles. Calculated from data in Fig. S1 of Reconditi et al. (2014).

subpeaks of the M3 reflection at longer sarcomere lengths (Fig. 2 B), and the experimental profile (black) is closer to that expected from the Brunello et al. (2007) model (magenta) than that expected by the modified model in which the detached motors make no contribution to the M3 reflection (green). However the limited signal-to-noise ratio of the outer peaks at longer sarcomere length precludes a quantitative determination of the degree of disorder of the nonoverlap motors.

From the physiological perspective of thick filament–based regulation in muscle, the most important implication of the modeling presented above is that the motors in the no-overlap region could not have remained in the folded conformation. That conclusion was not tested directly by Reconditi et al. (2014). To do so, we modified the model so that a fraction of the motors in the nonoverlap region remain in the folded state, with the axial mass distribution determined in resting muscle (Reconditi et al., 2011). We found that if as little as 10% of the motors in the no-overlap region were in the folded conformation, R_{M3} would increase with increasing sarcomere length (Fig. 1 B, blue), in contrast to the observed decrease (black). This result provides strong evidence that nearly all the myosin motors in the non-overlap region of the thick filament leave the folded conformation during isometric contraction.

Finally, we consider why Squire and Knupp (2021) reached a different conclusion, starting from apparently the same data. Those authors used a simpler structural model to calculate the axial profile of the M3 reflection, but their model is equivalent to that presented above in which, during contraction, the motors in the no-overlap region are assumed to make no contribution to the M3 reflection because they are completely disordered (Figs. 1 and 2, green). Reconditi et al. (2014) did not make that assumption, but rather used a published model in which these motors had an axial Gaussian mass dispersion of 3.6 nm (Figs. 1 and 2, magenta). We have already noted that the Reconditi et al. (2014) model gives a reasonable fit to the sarcomere length dependence of both the I_{M3} and the axial profile of the M3 reflection.

The main reason that Squire and Knupp reached a different conclusion using a similar theoretical framework, however, seems to be that they considered the contributions of only the central two subpeaks of the M3 reflection in their comparison with the experimental I_{M3} values of Reconditi et al. (2014), whereas we included all the subpeaks in both the experimental and model values of I_{M3}. Squire and Knupp appear to have assumed, incorrectly, that the experimental I_{M3} values of Reconditi et al. (2014) were determined from only the central two peaks. In a paragraph discussing the axial extent of the M3 reflection, they state "Reconditi et al (2014) say that the observed peak widths do not change with sarcomere length." In fact, Reconditi et al. (2014) show that it is the cross-meridional width that is constant in the relevant range of sarcomere length, whereas the axial width does increase with sarcomere length (Fig. 2). The relevant data for the cross-meridional width are reproduced here as Fig. 3 with an explicit calibration added in reciprocal nanometers.

Squire and Knupp's alternative explanation for the observed decrease in I_{M3} with increasing sarcomere length in the range of 2.1 to 2.6 μm is that it might be due to a decrease in the degree of alignment of neighboring thick filaments during isometric contraction at longer sarcomere lengths, and they base this explanation on theoretical diffraction patterns calculated from a hexagonal array of 25 "thick filaments" modeled as a three-start helix of spheres (Eakins et al., 2019). According to the authors, this model predicts that filament misalignment results in a decrease in intensity of the M3 reflection with no change at all in its cross-meridional width, a result reproduced as Fig. 4 b of Squire and Knupp (2021). However, this unexpected conclusion does not appear to be supported by the diffraction patterns calculated from the model (Fig. 7 in Eakins et al., 2019), which are themselves inconsistent with experimental measurements of the cross-meridional width of the M3 reflection following the classic studies of Huxley et al. (1982). Those authors showed that the cross-meridional width of the M3 reflection increases during contraction, and they interpreted that increase in terms of greater axial misalignment between neighboring thick filaments.

That result has been reproduced by many subsequent x-ray studies, and the interpretation has been confirmed by EM of rapidly frozen muscles (Sosa et al., 1994; Lenart et al., 1996). Therefore, it seems very likely that, in physiological conditions, any decrease in the degree of alignment between thick filaments would be accompanied by an increase in the cross-meridional width of the M3 reflection, an effect that is not observed at sarcomere lengths up to 2.6 µm (Fig. 3), in which the intensity of the reflection decreases linearly with increasing sarcomere length (Fig. 2 A). Squire and Knupp's alternative explanation of the decrease in the intensity of the M3 reflection at sarcomere lengths up to 2.6 µm therefore seems unlikely.

In summary, the original conclusion of Reconditi et al. (2014), that activation of fast-twitch skeletal muscle induces nearly all the myosin motors in the nonoverlap region of the thick filament to leave the folded conformation that they took up in the resting muscle, is confirmed by the additional analysis presented here. The signaling pathway which triggers that structural transition remains to be fully elucidated, but it cannot be a consequence of binding to an activated thin filament.

Acknowledgments

Henk L. Granzier served as editor.

We thank European Synchrotron Radiation Facility (ESRF) for provision of synchrotron beamtime, Mario Dolfi, the staff of the mechanical workshop of the Department of Physics and Astronomy (University of Florence), and Jacques Gorini (ESRF) for electronic and mechanical engineering support.

This work and some investigators were supported by Fondo per gli Investimenti della Ricerca di Base (Futuro in Ricerca project RBFR08JAMZ to E. Brunello, Italy); Progetti di Rilevante Interesse Nazionale-Ministero dell'Istruzione, dell'Università e della Ricerca (PRIN-MIUR), and Telethon (Italy); Fondazione Cassa di Risparmio di Firenze (2016-2018; Italy); UK Medical Research Council (grant MR/M026655/1); and the ESRF. E. Brunello was funded by a British Heart Foundation Intermediate Basic Science Research Fellowship FS/17/3/32604. L. Fusi was funded by a Sir Henry Dale Fellowship awarded by the Wellcome Trust and the Royal Society (fellowship 210464/Z/18/Z).

The authors declare no competing financial interests.

Author contributions: M. Reconditi, E. Brunello, L. Fusi, M. Linari, V. Lombardi, M. Irving and G. Piazzesi designed and performed research; M. Reconditi and G. Piazzesi analyzed data; M. Reconditi, E. Brunello, L. Fusi, M. Linari, V. Lombardi, M. Irving and G. Piazzesi wrote and contributed to critical revision of the paper.

References

AL-Khayat, H.A., R.W. Kensler, J.M. Squire, S.B. Marston, and E.P. Morris. 2013. Atomic model of the human cardiac muscle myosin filament. *Proc. Natl. Acad. Sci. USA.* 110:318–323. https://doi.org/10.1073/pnas.1212708110

Brunello, E., M. Reconditi, R. Elangovan, M. Linari, Y.B. Sun, T. Narayanan, P. Panine, G. Piazzesi, M. Irving, and V. Lombardi. 2007. Skeletal muscle resists stretch by rapid binding of the second motor domain of myosin to actin. *Proc. Natl. Acad. Sci. USA.* 104:20114–20119. https://doi.org/10.1073/pnas.0707626104

Brunello, E., L. Fusi, M. Reconditi, M. Linari, P. Bianco, P. Panine, T. Narayanan, G. Piazzesi, V. Lombardi, and M. Irving. 2009. Structural changes in myosin motors and filaments during relaxation of skeletal muscle. *J. Physiol.* 587:4509–4521. https://doi.org/10.1113/jphysiol.2009.176222

Brunello, E., L. Fusi, A. Ghisleni, S.J. Park-Holohan, J.G. Ovejero, T. Narayanan, and M. Irving. 2020. Myosin filament-based regulation of the dynamics of contraction in heart muscle. *Proc. Natl. Acad. Sci. USA.* 117:8177–8186. https://doi.org/10.1073/pnas.1920632117

Eakins, F., C. Knupp, and J.M. Squire. 2019. Monitoring the myosin cross-bridge cycle in contracting muscle: steps towards 'Muscle—the Movie.' *J. Muscle Res. Cell Motil.* 40:77–91. https://doi.org/10.1007/s10974-019-09543-9

Fusi, L., E. Brunello, Z. Yan, and M. Irving. 2016. Thick filament mechano-sensing is a calcium-independent regulatory mechanism in skeletal muscle. *Nat. Commun.* 7:13281. https://doi.org/10.1038/ncomms13281

Gordon, A.M., A.F. Huxley, and F.J. Julian. 1966. The variation in isometric tension with sarcomere length in vertebrate muscle fibres. *J. Physiol.* 184:170–192. https://doi.org/10.1113/jphysiol.1966.sp007909

Gordon, A.M., E. Homsher, and M. Regnier. 2000. Regulation of contraction in striated muscle. *Physiol. Rev.* 80:853–924. https://doi.org/10.1152/physrev.2000.80.2.853

Haselgrove, J.C. 1975. X-ray evidence for conformational changes in the myosin filaments of vertebrate striated muscle. *J. Mol. Biol.* 92:113–143. https://doi.org/10.1016/0022-2836(75)90094-7

Hooijman, P., M.A. Stewart, and R. Cooke. 2011. A new state of cardiac myosin with very slow ATP turnover: a potential cardioprotective mechanism in the heart. *Biophys. J.* 100:1969–1976. https://doi.org/10.1016/j.bpj.2011.02.061

Huxley, H.E. 1973. Muscular contraction and cell motility. *Nature.* 243:445–449. https://doi.org/10.1038/243445a0

Huxley, H.E., and W. Brown. 1967. The low-angle x-ray diagram of vertebrate striated muscle and its behaviour during contraction and rigor. *J. Mol. Biol.* 30:383–434. https://doi.org/10.1016/S0022-2836(67)80046-9

Huxley, H.E., A.R. Faruqi, M. Kress, J. Bordas, and M.H.J. Koch. 1982. Time-resolved X-ray diffraction studies of the myosin layer-line reflections during muscle contraction. *J. Mol. Biol.* 158:637–684. https://doi.org/10.1016/0022-2836(82)90253-4

Huxley, H., M. Reconditi, A. Stewart, and T. Irving. 2006. X-ray interference studies of crossbridge action in muscle contraction: evidence from quick releases. *J. Mol. Biol.* 363:743–761. https://doi.org/10.1016/j.jmb.2006.08.075

Irving, M. 2017. Regulation of contraction by the thick filaments in skeletal muscle. *Biophys. J.* 113:2579–2594. https://doi.org/10.1016/j.bpj.2017.09.037

Irving, M., G. Piazzesi, L. Lucii, Y.B. Sun, J.J. Harford, I.M. Dobbie, M.A. Ferenczi, M. Reconditi, and V. Lombardi. 2000. Conformation of the myosin motor during force generation in skeletal muscle. *Nat. Struct. Biol.* 7:482–485. https://doi.org/10.1038/75890

Lenart, T.D., J.M. Murray, C. Franzini-Armstrong, and Y.E. Goldman. 1996. Structure and periodicities of cross-bridges in relaxation, in rigor, and during contractions initiated by photolysis of caged Ca^{2+}. *Biophys. J.* 71:2289–2306. https://doi.org/10.1016/S0006-3495(96)79464-X

Linari, M., G. Piazzesi, I. Dobbie, N. Koubassova, M. Reconditi, T. Narayanan, O. Diat, M. Irving, and V. Lombardi. 2000. Interference fine structure and sarcomere length dependence of the axial x-ray pattern from active single muscle fibers. *Proc. Natl. Acad. Sci. USA.* 97:7226–7231. https://doi.org/10.1073/pnas.97.13.7226

Linari, M., E. Brunello, M. Reconditi, L. Fusi, M. Caremani, T. Narayanan, G. Piazzesi, V. Lombardi, and M. Irving. 2015. Force generation by skeletal muscle is controlled by mechanosensing in myosin filaments. *Nature.* 528:276–279. https://doi.org/10.1038/nature15727

Luther, P.K., H. Winkler, K. Taylor, M.E. Zoghbi, R. Craig, R. Padrón, J.M. Squire, and J. Liu. 2011. Direct visualization of myosin-binding protein C bridging myosin and actin filaments in intact muscle. *Proc. Natl. Acad. Sci. USA.* 108:11423–11428. https://doi.org/10.1073/pnas.1103216108

Parry, D.A., and J.M. Squire. 1973. Structural role of tropomyosin in muscle regulation: analysis of the x-ray diffraction patterns from relaxed and contracting muscles. *J. Mol. Biol.* 75:33–55. https://doi.org/10.1016/0022-2836(73)90527-5

Piazzesi, G., M. Reconditi, M. Linari, L. Lucii, Y.B. Sun, T. Narayanan, P. Boesecke, V. Lombardi, and M. Irving. 2002. Mechanism of force generation by myosin heads in skeletal muscle. *Nature.* 415:659–662. https://doi.org/10.1038/415659a

Reconditi, M. 2006. Recent improvements in small angle x-ray diffraction for the study of muscle physiology. *Rep. Prog. Phys.* 69:2709–2759. https://doi.org/10.1088/0034-4885/69/10/R01

Reconditi, M., M. Linari, L. Lucii, A. Stewart, Y.B. Sun, P. Boesecke, T. Narayanan, R.F. Fischetti, T. Irving, G. Piazzesi, et al. 2004. The myosin motor in muscle generates a smaller and slower working stroke at higher load. *Nature.* 428:578–581. https://doi.org/10.1038/nature02380

Reconditi, M., E. Brunello, M. Linari, P. Bianco, T. Narayanan, P. Panine, G. Piazzesi, V. Lombardi, and M. Irving. 2011. Motion of myosin head domains during activation and force development in skeletal muscle. *Proc. Natl. Acad. Sci. USA.* 108:7236–7240. https://doi.org/10.1073/pnas.1018330108

Reconditi, M., E. Brunello, L. Fusi, M. Linari, M.F. Martinez, V. Lombardi, M. Irving, and G. Piazzesi. 2014. Sarcomere-length dependence of myosin filament structure in skeletal muscle fibres of the frog. *J. Physiol.* 592: 1119–1137. https://doi.org/10.1113/jphysiol.2013.267849

Reconditi, M., M. Caremani, F. Pinzauti, J.D. Powers, T. Narayanan, G.J. Stienen, M. Linari, V. Lombardi, and G. Piazzesi. 2017. Myosin filament activation in the heart is tuned to the mechanical task. *Proc. Natl. Acad. Sci. USA.* 114:3240–3245. https://doi.org/10.1073/pnas.1619484114

Shaffer, J.F., R.W. Kensler, and S.P. Harris. 2009. The myosin-binding protein C motif binds to F-actin in a phosphorylation-sensitive manner. *J. Biol. Chem.* 284:12318–12327. https://doi.org/10.1074/jbc.M808850200

Sosa, H., D. Popp, G. Ouyang, and H.E. Huxley. 1994. Ultrastructure of skeletal muscle fibers studied by a plunge quick freezing method: myofilament lengths. *Biophys. J.* 67:283–292. https://doi.org/10.1016/S0006-3495(94)80479-5

Squire, J.M., and C. Knupp. 2021. Analysis methods and quality criteria for investigating muscle physiology using x-ray diffraction. *J. Gen. Physiol.* 153:e202012778. https://doi.org/10.1085/jgp.202012778

Stewart, M.A., K. Franks-Skiba, S. Chen, and R. Cooke. 2010. Myosin ATP turnover rate is a mechanism involved in thermogenesis in resting skeletal muscle fibers. *Proc. Natl. Acad. Sci. USA.* 107:430–435. https://doi.org/10.1073/pnas.0909468107

Wendt, T., D. Taylor, K.M. Trybus, and K. Taylor. 2001. Three-dimensional image reconstruction of dephosphorylated smooth muscle heavy meromyosin reveals asymmetry in the interaction between myosin heads and placement of subfragment 2. *Proc. Natl. Acad. Sci. USA.* 98:4361–4366. https://doi.org/10.1073/pnas.071051098

Woodhead, J.L., F.Q. Zhao, R. Craig, E.H. Egelman, L. Alamo, and R. Padrón. 2005. Atomic model of a myosin filament in the relaxed state. *Nature.* 436:1195–1199. https://doi.org/10.1038/nature03920

Yamada, Y., K. Namba, and T. Fujii. 2020. Cardiac muscle thin filament structures reveal calcium regulatory mechanism. *Nat. Commun.* 11:153. https://doi.org/10.1038/s41467-019-14008-1

Zoghbi, M.E., J.L. Woodhead, R.L. Moss, and R. Craig. 2008. Three-dimensional structure of vertebrate cardiac muscle myosin filaments. *Proc. Natl. Acad. Sci. USA.* 105:2386–2390. https://doi.org/10.1073/pnas.0708912105